Telecommunications and Radio Engineering, 74 (16):1483-1483 (2015)

VERTICAL PROFILE OF ATMOSPHERIC CONDUCTIVITY CORRESPONDING TO SCHUMANN RESONANCE PARAMETERS *

A.P. Nickolaenko[1♦], Yu.P. Galuk[2], & M. Hayakawa [3]

[1]*A.Ya. Usikov Institute for Radiophysics and Electronics of the National Academy of Sciences of Ukraine 12, Academician Proskura St., Kharkiv 61085, Ukraine*

[2]*Saint-Petersburg State University, 7/9 Universitetskaya nab., St. Petersburg, 199034, Russia*

[3] *Hayakawa Institute of Seismo Electromagnetics Co. Ltd. UEC Incubation Center-508, 1-5-1 Chofugaoka, Chofu Tokyo 182-8585, Japan*

♦Address all correspondence to A.P. Nickolaenko E-mail: sasha@ire.kharkov.ua

The search for a realistic vertical conductivity profile of atmosphere remains an update task of great importance for the direct electromagnetic simulations of global electromagnetic (Schumann) resonance. Such a profile is necessary when describing the impact on the ionosphere of the space weather, the pre-seismic activity or other various factors. Knowledge of the regular conductivity profile is of particular importance, since it allows computing of the observed regular parameters of Schumann resonance. Starting from the classic data, we developed the new height conductivity profile of atmosphere in the range from 2 to 98 km. The profile allows obtaining the Schumann resonance parameters consistent with experimental observations. The propagation constant of extremely low frequencies (ELF) radio waves was computed corresponding to this profile by using the rigorous full wave solution. We demonstrate a high correspondence of the frequency dependence obtained to the conventional reference model based on the records of global electromagnetic resonance. The conductivity profiles are also suggested for the ambient day and ambient night conditions. We obtained the propagation constants relevant to these profiles using the full wave solution. The power spectra of Schumann resonance were also computed and compared of the vertical electric field component in the case of uniform global distribution of thunderstorms. Spectra relevant to suggested conductivity profiles were compared with the spectrum obtained in the frameworks of the standard reference model. We also show consistency of the model data obtained with the conductivity profiles with the results of measurements of the radio signals radiated by ELF transmitters.

KEY WORDS: *vertical profile of atmospheric conductivity, propagation constant of ELF radio waves, power spectra of the Schumann resonance, ELF attenuation of radio waves emitted by ELF transmitters*

* Originally published in *Radiophysics and Electronics*, Vol. 6(20), No 3, 2015, pp. 30–37.

1. INTRODUCTION

The standard description of the sub-ionospheric extremely low frequency radio propagation (ELF: 3 Hz-3 kHz) implies the propagation constant $\nu(f)$, the source-observer distance θ, and the point source current moment $Ids(f)$. The propagation constant $\nu(f)$ plays an exceptionally important role in computations and simulations, therefore, special attention is directed to its precise derivation (see e.g. [1,2] and reference therein). The conventional standard or reference model of the propagation constant was introduced in paper [3], which summarized the extensive ensemble of experimental data collected by the Schumann resonance observatories. The field sites were positioned both in Eastern and the Western hemispheres. The complex propagation constant $\nu(f)$ is calculated in the model [3] from the following equations:

$$\nu(f) = \left[0.25 + (kaS)^2\right]^{1/2} - 0.5, \tag{1}$$

where a is the Earth's radius, k is the wave number in the free space, and f is the frequency,

$$S = c/V - i5.49\alpha / f; \tag{2}$$

is the so-called "complex sine" function with the following real and imaginary parts

$$c/V = 1.64 - 0.1759\ln(f) + 0.01791\left[\ln(f)\right]^2; \tag{3}$$

$$\alpha = 0.063 f^{0.64}. \tag{4}$$

Comparison of the experimental Schumann resonance data with those computed from equations (1)–(4) demonstrated a high quality of the model [3], although, some other $\nu(f)$ models are also used in literature, e.g., [1,2]. We use relations (1)–(4) as the standard or reference model.

Knowledge of the vertical profile of atmospheric conductivity $\sigma(h)$ is not obligatory when computing electromagnetic fields and interpreting the experimental data. It is sufficient to turn to the customary formula for the field components, which include the propagation constant, the current moment of the field source, the source–observer distance, and the effective height of the ionosphere [1,2].

The conductivity profile and the relevant complex permittivity of the air become obligatory when applying the direct computation techniques, such as finite dimension time domain (*FDTD*) method or the 2D telegraph equation (*2DTE*) [4–9]. The height interval from about 50 to 100 km is crucial for the sub-ionospheric ELF radio propagation, and this area is inaccessible for the modern means of remote sensing. The available experimental data on the air conductivity at these altitudes are rare, and there were obtained by rocket probing. Therefore, one can find only a few experimental altitude profiles of air conductivity in the literature. It is important to remark that none of these profiles gives the reference $\nu(f)$ frequency dependence (1)–(4).

The objective of this paper is derivation of a realistic $\sigma(h)$ profile that corresponds to the observed Schumann resonance parameters. This kind of model is especially desirable for the modeling of sub-ionospheric ELF radio wave propagation in the real Earth–ionosphere cavity.

2. AIR CONDUCTIVITY AS A FUNCTION OF ALTITUDE

We start from the classical work [10] when developing the height dependence $\sigma(h)$ corresponding to the observed resonance frequencies and the quality factors of Schumann resonance. The paper [10] proposed the conductivity profiles based on observational results and on the data of aeronomy. These profiles are still often used in many modern investigations. Curve with dots (line 1) in Fig. 1 shows the profile adopted from [10]. The main obstacle preventing its direct application in the Schumann resonance studies is the unrealistic value of the ELF radio propagation constant. As a result, the computed Schumann resonance spectra apparently deviate from observations. We developed profile 2 shown in Fig. 1, which gives much more realistic data. Simultaneously, this profile is rather close to the classical dependence [10], and hence, it agrees both with the contact measurements of the air conductivity and with the aeronomical data. Table 1 lists the logarithm of conductivity (in S/m) versus the altitudes above the ground (in km).

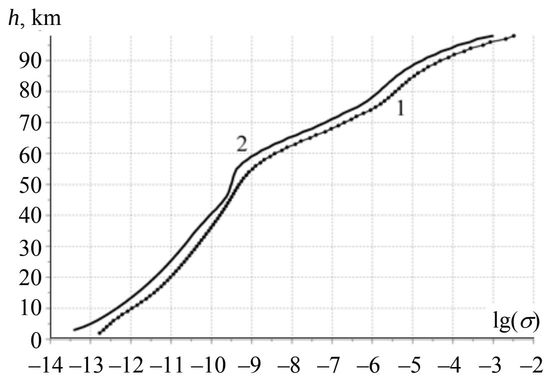

FIG. 1: Height profiles of the atmospheric conductivity: curve 1 is the classic profile [10], curve 2 is the new profile matching the Schumann resonance observations

Figure 1 shows atmospheric conductivity in the altitude range from 0 to 100 km. Here, curve 1 (with dots) depicts the classic profile [10], and the smooth curve 2 is the new more realistic profile $\sigma(h)$. As one can observe, the both curves are rather close to each other. Although, profile 2 has more pronounced changes between 50 and 60 km (the so-called “knee area”). Deviations begin around 30 km altitude, so that profile 2 becomes elevated over the classical $\sigma(h)$ dependence.

The heuristic “knee model” is often used in the Schumann resonance studies suggested in [11] replacing the reference model (1)–(4) in computations of the $\nu(f)$ propagation constant. Similarly to previous works [4–6,12–16], the knee model postulates a set of parameters that allow computing the complex characteristic heights (the electric and magnetic) and the real (non-complex) scale heights of the conductivity profiles relevant to these heights. The propagation constant is calculated by substituting these characteristic heights and the height scales into the heuristic equations, and the frequency dependence of all model parameters is separately postulated [11]. After obtaining the ELF propagation constant, one can turn to the field computations [2,17].

Unfortunately, every work exploiting the knee model operates only with the verbal description of the relevant conductivity profile, and none of them depicts the altitude dependence $\sigma(h)$ corresponding to the specific model parameters. Simultaneously, constructing of such a profile is a difficult task, provided that this is possible at all. One of the reasons is that the knee model parameters dependent on frequency. It is not clear therefore in what a way one can apply the complex functions of frequency when obtaining the real function of height $\sigma(h)$ corresponding to the particular knee model, which is independent of frequency. In any case, this problem is still not solved.

Simplified height profiles of conductivity are widely used in the direct field computations. These profiles typically correspond to the lg[$\sigma(h)$] plot formed by the straight line bent in the vicinity of the knee altitude. The kink is conditioned by the change in the profile scale height [8,9,18–20]. Such a height dependence of conductivity is in fact the well-known two-scale exponential model [21]. Disadvantages of such two-scale models are well-known and were discussed in detail in [11,21,22].

3. PROPAGATION CONSTANT

The ELF propagation constant $\nu(f)$ is constructed under an assumption that isotropic ionosphere plasma is horizontally homogeneous. One can compute the $\nu(f)$ dependence corresponding to the particular $\sigma(h)$ profile by using the full wave solution (*FWS*), as it was described in [23–27]. The full wave solution is the rigorous solution of radio propagation problem in the stratified ionosphere. The passed and the reflected waves are used in each horizontal layer. The thickness of a layer is much smaller than the wavelength in the medium. The tangential field components remain continuous at interfaces of layers. In might be shown [23-27] that this boundary problem might be reduced to the first order nonlinear differential equation (Riccati equation), provided that the surface impedance is introduced being the ratio of the tangential components of E_t and H_t. The obtained Riccati equation is solved numerically by the successive approximations. As a result, one obtains the propagation constant $\nu(f)$ sought. The term “full wave solution” is used, since all the field components are rigorously accounted for that propagate in the stratified plasma and in the air.

TABLE 1: Logarithm of atmospheric conductivity (S/m) as function of altitude above the ground

z, km	**lg(σ)**			**z, km**	**lg(σ)**			**z, km**	**lg(σ)**		
	Night	**Day**	**Average**		**Night**	**Day**	**Average**		**Night**	**Day**	**Average**
2	–13,82	–13,82	–13,82	34	–10,39	–10,24	–10,39	66	–8,24	–7,17	–7,73
3	–13,67	–13,67	–13,67	35	–10,32	–10,16	–10,32	67	–8,10	–7,02	–7,50
4	–13,40	–13,40	–13,40	36	–10,25	–10,09	–10,25	68	–7,90	–6,85	–7,35
5	–13,17	–13,17	–13,17	37	–10,18	–9,97	–10,18	69	–7,73	–6,72	–7,17
6	–12,99	–12,99	–12,99	38	–10,11	–9,92	–10,11	70	–7,50	–6,55	–7,02
7	–12,84	–12,84	–12,84	39	–10,04	–9,84	–10,04	71	–7,35	–6,37	–6,85
8	–12,71	–12,71	–12,71	40	–9,99	–9,75	–9,97	72	–7,17	–6,25	–6,72
9	–12,58	–12,58	–12,58	41	–9,93	–9,69	–9,88	73	–7,02	–6,12	–6,55
10	–12,46	–12,46	–12,46	42	–9,87	–9,63	–9,82	74	–6,85	–6,02	–6,37
11	–12,35	–12,35	–12,35	43	–9,81	–9,59	–9,75	75	–6,72	–5,93	–6,25
12	–12,24	–12,24	–12,24	44	–9,75	–9,56	–9,69	76	–6,55	–5,83	–6,12
13	–12,13	–12,13	–12,13	45	–9,68	–9,53	–9,63	77	–6,37	–5,76	–6,02
14	–12,03	–12,03	–12,03	46	–9,64	–9,51	–9,9	78	–6,25	–5,66	–5,93
15	–11,93	–11,93	–11,93	47	–9,62	–9,48	–9,56	79	–6,12	–5,58	–5,83
16	–11,84	–11,84	–11,84	48	–9,58	–9,46	–9,53	80	–6,02	–5,49	–5,76
17	–11,74	–11,74	–11,74	49	–9,57	–9,44	–9,51	81	–5,93	–5,41	–5,66
18	–11,65	–11,65	–11,65	50	–9,56	–9,40	–9,48	82	–5,83	–5,29	–5,58
19	–11,57	–11,57	–11,57	51	–9,53	–9,38	–9,46	83	–5,76	–5,19	–5,49
20	–11,48	–11,48	–11,48	52	–9,51	–9,29	–9,44	84	–5,66	–5,05	–5,41
21	–11,40	–11,40	–11,40	53	–9,48	–9,22	–9,41	85	–5,58	–4,94	–5,29
22	–11,32	–11,32	–11,32	54	–9,46	–9,10	–9,38	86	–5,49	–4,77	–5,19
23	–11,24	–11,24	–11,24	55	–9,44	–9,01	–9,29	87	–5,41	–4,64	–5,05
24	–11,17	–11,17	–11,17	56	–9,40	–8,86	–9,22	88	–5,29	–4,43	–4,94
25	–11,10	–11,10	–11,10	57	–9,38	–8,75	–9,10	89	–5,19	–4,29	–4,77
26	–11,03	–11,03	–11,03	58	–9,29	–8,57	–9,01	90	–5,05	–4,04	–4,64
27	–10,96	–10,96	–10,96	59	–9,22	–8,45	–8,86	91	–4,94	–3,89	–4,43
28	–10,89	–10,89	–10,89	60	–9,10	–8,24	–8,75	92	–4,77	–3,58	–4,29
29	–10,82	–10,82	–10,82	61	–9,01	–8,10	–8,57	93	–4,64	–3,40	–4,04
30	–10,76	–10,74	–10,76	62	–8,86	–7,87	–8,45	94	–4,43	–3,01	–3,89
31	–10,69	–10,65	–10,69	63	–8,75	–7,73	–8,24	95	–4,29	–2,81	–3,58
32	–10,63	–10,58	–10,63	64	–8,57	–7,50	–8,10	96	–4,04	–2,61	–3,40
33	–10,57	–10,51	–10,57	65	–8,45	–7,35	–7,87	97	–3,89	–2,41	–3,01
								98	–3,58	–2,21	–2,81

Figure 2 compares two frequency dependent complex $\nu(f)$ functions. The real and imaginary parts of the reference propagation constant were computed using the (1)–(4) formulas, and the second kind functions were obtained in the rigorous *FWS* solution for the profiles 1 and 2 shown in Fig. 1. The absolute inaccuracy in the $\nu(f)$ did not exceed 10^{-7} obtained by computations with the successive approximation in the full wave solution.

All models provide the close values of the real part of propagation constant (the phase velocity of radio waves): these deviate by a few percents. Therefore, the resonance frequencies are almost equal when found in all three models. Departures in the imaginary part or in the radio wave attenuation are more apparent. The standard reference model and the conductivity profile 2 give the close frequency dependence (curves 4 and 6). Attenuation computed for the classical conductivity profile [10] (curve 5) appreciably deviates from the reference curve.

Relative deviations of the real part (curve 1) and the imaginary part (curve 2) of the propagation constant are shown in Fig. 3. Curve 1 corresponds to deviations in the real part of the propagation constant, defined by equation (5), and curve 2 shows departures in the imaginary part, described by formula (6):

$$\delta_R = 100\left\{\mathrm{Re}\left[\nu_2(f)\right] - \mathrm{Re}\left[\nu_0(f)\right]\right\}\big/\mathrm{Re}\left[\nu_0(f)\right]; \tag{5}$$

$$\delta_I = 100\left\{\mathrm{Im}\left[\nu_2(f)\right] - \mathrm{Im}\left[\nu_0(f)\right]\right\}\big/\mathrm{Im}\left[\nu_0(f)\right]. \tag{6}$$

Here, $\nu_0(f)$ is the reference model defined by formulas (1)–(4), and $\nu_2(f)$ is the propagation constant found by the full wave solution for the conductivity profile 2.

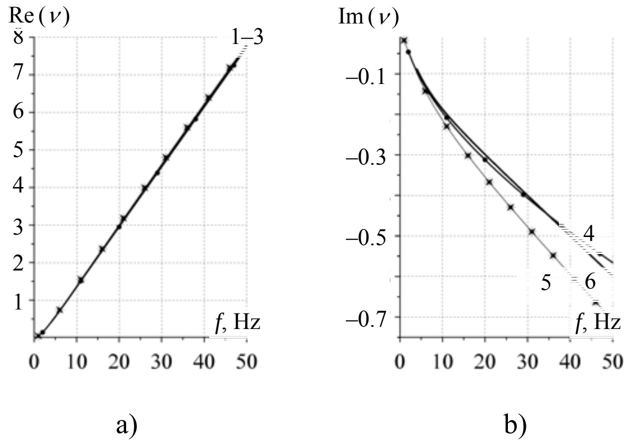

FIG. 2: Dispersion curves: a) the real part of propagation constant: lines 1-3 show the Re[$\nu(f)$] for model [3], the classical profile [10], and the new conductivity profile correspondingly; b) the imaginary part of propagation constant: line 4 is the reference model [3], line 5 depicts data for the classic profile [10], line 6 presents results for the new profile

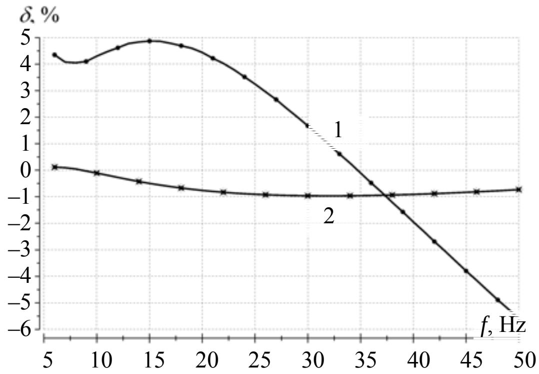

FIG. 3: Relative deviation of the real (curve 1) and the imaginary (curve 2) parts the propagation constant obtained for profile 2 with respect to the reference model [3]

Plots in Fig. 3 show that profile 2 gives the propagation constant close to the reference dependence in the entire frequency range of Schumann resonance: deviations in the phase velocity of ELF radio waves do not exceed 1% and those in the wave attenuation are below 5%. Therefore, one can use this profile with parameters listed in Table 1 for modeling the global electromagnetic resonance in the Earth–ionosphere cavity regardless the particular computational technique including the direct field calculations, such as the *FDTD*.

Validity of the proposed conductivity profile can be additionally confirmed by comparing the calculated attenuation rate with its direct measurements conducted using the narrow-band signal arriving from the ELF transmitters [28–30]. Data of paper [28] are based on the systematic monitoring of the signal amplitude arriving form the US Navy ELF transmitter regarded as Wisconsin Test Facility (*WTF*). Measurements were performed at the globally distributed field sites and correspond to the 76 Hz frequency. Here, the observed wave attenuation was equal to 0.82 dB/Mm in ambient night and to 1.33 dB/Mm in the ambient day conditions (1 Mm = 1000 km). Average attenuation rate at this frequency is equal to 1.08 dB/Mm. The relative standard deviation of observational data was evaluated by ±25% value with an account for seasonal trends.

The proposed profile 2 provides the imaginary part of propagation constant Im[(*f*)] = 0.86 at this frequency, which corresponds to the attenuation rate of 1.17 dB/Mm. On our opinion, the attenuation rate thus obtained is practically coincident with the observational data, which undoubtedly confirms the accuracy of the new profile model.

Papers [29] provide the imaginary part of the propagation constant that was measured at 82 Hz frequency being equal to $\mathrm{Im}[\nu(f)]|_{f=82} = 0.9225$. It corresponds to the radio wave attenuation rate $\alpha = 1.25$ dB/Mm, which was obtained from the distance dependence of the vertical electric field amplitude of the signal radiated by the Kola Peninsula Transmitter (CPT) of the Soviet Navy. Thus, the model imaginary part of the propagation constant is equal to $\mathrm{Im}[\nu(f)]|_{f=82}=$ 0.9162. Again, this value is practically coincident with the experimentally measured quantity. Thus, comparison with experimental observations of the man-made ELF radio signals provides an additional confirmation of the applicability of the proposed conductivity profile (see Table 2).

4. POWER SPECTRA

To demonstrate correspondence of results obtained by using the proposed profile to the reference model [3], we computed the power spectra of the vertical electric field component shown in Fig. 4. To eliminate the distance dependence in the spectral outline (the source–observer distance) from the model data, we assumed that the world thunderstorms are uniformly distributed over the globe [17]. In this case, the power spectrum is described by the following formula [1,2]:

$$\left|E(f)\right|^2 \propto \left|Ids(\omega)\frac{\nu(\nu+1)}{\omega}\right|^2 \sum_{n=0}^{\infty} \frac{2(2n+1)}{\left|n(n+1)-\nu(\nu+1)\right|^2}. \tag{7}$$

Here $\omega = 2\pi f$ is the circular frequency, n = 1, 2, 3... is the Schumann resonance mode number, $Ids(\omega)$ is the current moment of the source, we assume that it is a constant in the frequency band of Schumann resonance.

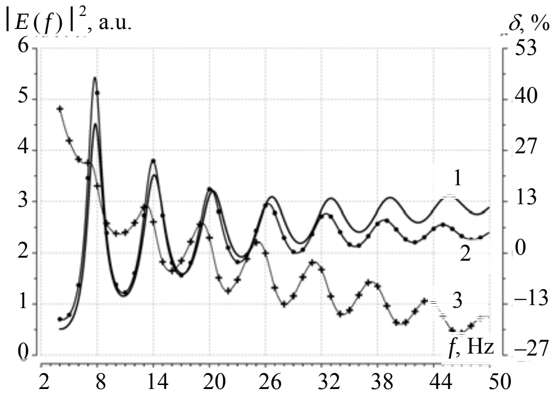

FIG. 4: The computed Schumann resonance spectra for the globally uniform distribution of lightning strikes: curve 1 shows the power spectrum of the vertical electric field obtained for profile 2 of Fig. 1; curve 2 depicts the spectrum calculated for the reference model' line 3 demonstrates relative deviations (in %) from the reference spectrum (shown on the right ordinate)

Figure 4 shows two resonance spectra. Curve 1 shows the computational data for the suggested vertical conductivity profile of atmosphere and curve 2 is the spectrum relevant to the reference frequency dependence of propagation constant [3]. Relative deviations from the reference spectrum are shown in percents by curve 3, which is constructed against the right ordinate. By comparing Figs. 3 and 4, we observe that deviations of two models become more apparent in the power spectra than in the dispersion curves $\nu(f)$. Even small deviations of the phase velocity of the ELF radio waves being about 1% are clearly visible in the spectra: one observes substantial departures of the peak frequencies, especially at higher modes. Curve 3 in Fig. 4 illustrates the relative deviations of the power spectra relevant for the new conductivity profile. Departures are in the range from −5 to 15% throughout the Schumann resonance band. These values are 3–4 times smaller than deviations relevant to the classical conductivity profile [3].

5. THE DAY–NIGHT NON-UNIFORMITY

The new conductivity profile is consistent with the Schumann resonance observations and the attenuation rate measurements by using the ELF radio transmissions. This allows us to go further and introduce the $\sigma(h)$ functions corresponding to the ambient day and night conditions. Corresponding plots are shown in Fig. 5.

The logarithm of the air conductivity is shown along the abscissa of Fig. 5, and the height above the ground is potted in km along the ordinate. The smooth line 2 in this figure reproduces the $\sigma(h)$ profile shown by line 2 in Fig. 1. Curve 1 in Fig. 5 corresponds to the nighttime conductivity when the ionosphere becomes elevated above the ground, and curve 3 is the daytime profile.

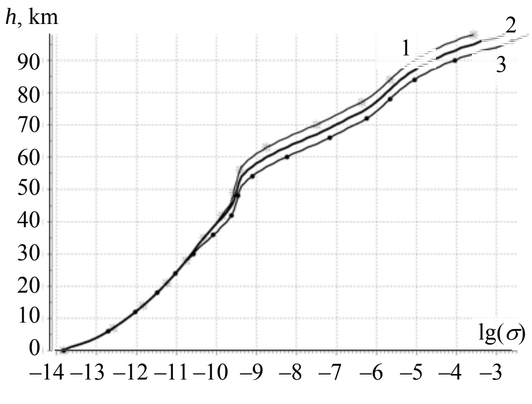

FIG. 5: Vertical conductivity profiles of atmosphere: Curve 1 corresponds to the daytime conditions, line 2 is the average profile, and curve 3 is the profile for the ambient nighttime conditions

By using the full wave solution, we computed the frequency dependence of the complex propagation constant for the daytime and nighttime conditions and compared these data with the reference model. After obtaining the propagation constants, we computed the power spectra of resonance oscillations in the ambient "day" and ambient "night" conditions. We will not address here the effect of the ionosphere day–night non-uniformity on the global electromagnetic resonance. The term "ambient day conditions" means that the horizontally homogeneous ionosphere is described by the same daytime conductivity profile all around the globe. Similarly, the words "night conditions" mean that the night profile of the ionosphere is used over all points above the Earth.

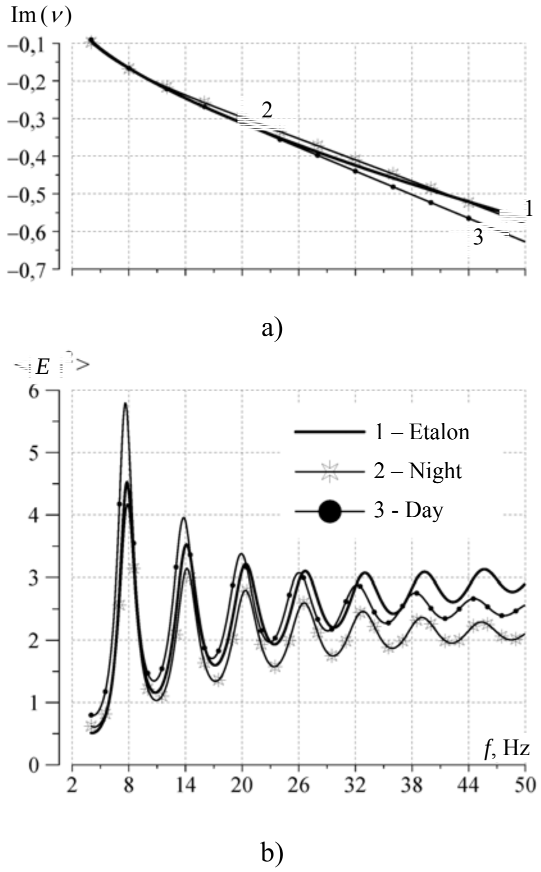

FIG. 6: Radio wave attenuation (a) and the computed the Schumann resonance power spectra of the vertical electric field component (b) computed for the uniform distribution of sources

Again, for eliminating the influence of the source–observer distance on the spectral data, we use the globally uniform distribution of the field sources. It is obvious that the "day" and the "night" spectra thus obtained describe two extreme situations of the “whole day” or the “whole night” cavity models. The power spectrum in the real cavity with the "day–night" non-uniformity will be found between these two extreme curves.

Figure 6 depicts calculated data for the day and the night conductivity profiles. The graphs of Fig. 6(a) clearly show that the reference attenuation factor (curve 1) lies between the values obtained for the night (curve 2) and the day (curve 3) conductivity profile in the whole Schumann resonance range. The graphs are shown in Fig. 6(b) of the power spectra of the vertical electric field.

As it could be expected, the resonance peaks in the power spectrum of the “whole night” resonator occur at the higher frequencies than peaks of the “whole day” cavity. The power spectrum of the reference propagation constant occupies the intermediate position between the day and night spectra. Thus, computations of the power spectra confirm the feasibility of the day and night conductivity profiles.

6. DISCUSSION OF RESULTS

The new height profile of atmospheric conductivity is close to the classical concept and, simultaneously, it agrees with observations of global electromagnetic resonance. Realistic frequency dependence of the frequency propagation constant was obtained by using the rigorous full wave solution of electromagnetic problem with the new conductivity profile. Thus, the model corresponds to the reference function used in the Schumann resonance frequency band. On the other hand, the model provides values very close to the attenuation rates observed in the records of man-made ELF radio signals at frequencies above the Schumann resonance [28,29]. We provide the relevant data in Table 2.

TABLE 2: Radio wave attenuation measured experimentally at particular frequencies and computed with the help of conductivity profiles

Data e	**$\langle\mathrm{Im}(\nu)\rangle$**	**$\langle\alpha\rangle$, dB/Mm**	**$\mathrm{Im}(\nu)$, Day**	**α, day, dB/Mm**	**$\mathrm{Im}(\nu)$, Night**	**α, night, dB/Mm**
f = 76 Hz, model	0.86	1.17	0.96	1.31	0.75	1.02
f = 76 Hz, experiment [28]	–	1.08	–	1.33	–	0.82
f = 82 Hz, model	0.92	1.25	1.01	1.38	0.79	1.08
f = 82 Hz, experiment [29,30]	–	1.26	–	–	–	–

Table 2 compares the computed data on the wave attenuation obtained for the conductivity profile presented in Table 1 with the published results on the radio emissions by ELF transmitters. Data at 76 Hz frequency were picked from the review article [28], which summarized results of the long-term observations of signals radiated by the US Navy transmitter (*WTF*) at different field sites. Results at the 82 Hz frequency were obtained from the distance dependence of the signal amplitude arriving from the Kola Peninsula Soviet Navy radio transmitter [29]. It is necessary to clarify here that the model computations provide the attenuation data in the dimensionless form of $\mathrm{Im}(\nu)$ measured in Napier/radians. The wave attenuation rate is measured experimentally in dB/Mm. These quantities are related by the following equation:

$$\alpha = \pi \lg(e)\mathrm{Im}(\nu) \approx 1.346\mathrm{Im}(\nu). \tag{8}$$

The model values $\mathrm{Im}(\nu)$ were re-arranged in Table 2 according to formula (8) for obtaining the wave attenuation in dB/Mm. As might be seen from Table 2, the average model attenuation at 76 Hz frequency is equal to 1.17 dB/Mm. The experimentally measured value is equal to 1.08 dB/Mm. Hence, the deviation is about 7%. Relative departures of the model from the measured attenuation rate in the day and in the night conditions are equal to 2 and 24% correspondingly.

At the 82 Hz frequency, the model and observed attenuation rates are practically coincident being 1.25 dB/Mm with the mutual deviation of less than 1%. One may conclude that the new vertical profile of atmospheric conductivity is consistent both in the range of the global electromagnetic resonance and also at frequencies of ELF radio communications (above the resonance).

7. CONCLUSIONS

The analysis performed and comparison of the results obtained with the available literature data suggest that the new vertical profile of atmospheric conductivity is close to reality.

1. It is consistent with the classical concept of the air ionization.
2. Its applications in the full wave solution provides the realistic frequency dependence of the propagation constant being close to the reference one.
3. The propagation constant obtained is in a good agreement with the measurements of man-made ELF radio signals.

REFERENCES

1. Nickolaenko, A.P. and Hayakawa, M., (2002), *Resonances in the Earth-ionosphere cavity*, Dordrecht-Boston-L.: Kluwer Academic Publ., – 380 p.
2. Nickolaenko, A. and Hayakawa, M., (2014), *Schumann resonance for tyros (Essentials of Global Electromagnetic Resonance in the Earth–Ionosphere Cavity)*, Tokyo-Heidelberg-N. Y.-Dordrecht-L.: Springer, 2014. – Ser. XI. Springer Geophysics. – 348 p.
3. Ishaq, M. and Jones, D.Ll., (1977), Method of obtaining radiowave propagation parameters for the Earth–ionosphere duct at ELF, *Electronic Lett*. **13**(2):254–255.
4. Kirillov, V.V., Kopeykin, V.N., and Mushtak, V.C., (1997), Electromagnetic waves of ELF band in the Earth–ionosphere cavity, *Geomagnetism and Aeronomy*. **37**(3):114–120 (in Russian).
5. Kirillov, V.V., (1996), 2D theory of ELF electromagnetic wave propagation in the Earth–ionosphere cavity, *Izv. VUZOV, Radiofizika*. **39**(12):1103–1112 (in Russian).

6. Kirillov, V.V. and Kopeykin, V.N., (2002), Solution of 2D telegraph equations with anisotropic parameters, *Izv. VUZOV, Radiofizika*. **45**(12):1011–1024 (in Russian).
7. Pechony, O. and Price, C., (2004), Schumann resonance parameters calculated with a partially uniform knee model on Earth, Venus, Mars, and Titan, *Radio Sci*. **39**(5):RS5007 (10 p.).
8. Yang, H. and Pasko, V.P., (2005), Three-dimensional finite-difference time domain modeling of the Earth-ionosphere cavity resonances, *Geophys. Res. Lett*. **32**(3):L03114 (4 p.).
9. Morente, J.A., Molina-Cuberos, G.J., Porti, J.A. et al., (2003), A numerical simulation of Earth's electromagnetic cavity with the Transmission Line Matrix method: Schumann resonances, *J. Geophys. Res*. **108**(A5):SIA 17-1–17-11.
10. Cole, R.K. and Pierce, E.T., (1965), Electrification in the Earth's atmosphere from altitudes between 0 and 100 kilometers, *J. Geophys. Res*. **70**(11):2735–2749.
11. Mushtak, V.C. and Williams, E., (2002), Propagation parameters for uniform models of the Earth-ionosphere waveguide, *J. Atmos. Solar-Terr. Phys*. **64**(6):1989–2001.
12. Greifinger, C. and Greifinger, P., (1978), Approximate method for determining ELF eigenvalues in the Earth−ionopshere waveguide, *Radio Sci*. **13**(5):831−837.
13. Nickolaenko, A.P. and Rabinowicz, L.M., (1982), On a possibility of global electromagnetic resonances at the planets of Solar system, *Kosmicheskie Issled*. **20**(1):82–89 (in Russian).
14. Nickolaenko, A.P. and Rabinowicz, L.M., (1987), On applicability of ELF global resonances for studing thunderstorm activity at Venus, *Kosmicheskie Issled*. **25**(2):301–306 (in Russian).
15. Sentman, D.D., (1990), Electrical conductivity of Jupiter Shallow interior and the formation of a resonant planetary-ionospheric cavity, *ICARUS*. **88**(1):73–86.
16. Füllekrug, M., (2000), Dispersion relation for spherical electromagnetic resonances in the atmosphere, *Phys. Lett. A*. **275**(1–2):80–89.
17. Williams, E.R., Mushtak, V.C., and Nickolaenko, A.P., (2006), Distinguishing ionospheric models using Schumann resonance spectra, *J. Geophys. Res*. **111**(D16):D16107 (12 p.).
18. Toledo-Redondo, S., Salinas, A., Morente-Molinera, J.A. et al., (2013), Parallel 3D-TLM algorithm for simulation of the Earth-ionosphere cavity, *J. Computational Phys*. **236**(3):367–379.
19. Molina-Cuberos, G.J., Morente, J.A., Besser, B.P. et al., (2006), Schumann resonances as a tool to study the lower ionospheric structure of Mars, *Radio. Sci*. **41**(1):RS1003 (8 p.).
20. Zhou, H., Yu, H., Cao, B., Qiao, X., (2013), Diurnal and seasonal variations in the Schumann resonance parameters observed at Chinese observatories, *J. Atmos. Solar-Terr. Phys*. **98**(1):86–96.
21. Sentman, D.D., (1990), Approximate Schumann resonance parameters for a two-scale-height ionosphere, *J. Atmos. Terr. Phys*. **52**(1):35–46.
22. Greifinger, P.S., Mushtak, V.C., and Williams, E.R., (2007), On modeling the lower characteristic ELF altitude from aeronomical data, *Radio Sci*. **42**(2):RS2S12 (12 p.).
23. Hynninen, E.M. and Galuk, Yu.P., (1972), Field of vertical dipole over the spherical Earth with non-uniform along height ionosphere, *Problems of diffraction and radio wave propagation*. 11:109–120 (in Russian).
24. Bliokh, P.V., Galuk, Yu.P., Hynninen, E.M., Nickolaenko, A.P. et al., (1977), On the resonance phenomena in the Earth-ionosphere cavity, *Radiophysics and Quantum Electronics*. **20**(4):339–345, doi:10.1007/BF01033918 (in Russian).
25. Bliokh, P.V., Nickolaenko, A.P., and Filippov, Yu.F., (1980), *Schumann resonances in the Earth−ionosphere cavity*, Peter Perigrinus, New York, - 168 p.
26. Galuk, Yu.P. and Ivanov, V.I., (1978), Deducing the propagation charactericics of VLF fields in the cavity Earth–non-uinform along the height anisotropic ionosphere, *Problems of diffraction and radio wave propagation*. 16:148–153 (in Russian).
27. Galuk, Yu.P., Nickolaenko, A.P., and Hayakawa, M., (2015), Comparison of exact and approximate solutions of the Schumann resonance problem for the knee conductivity profile, *Telecommunications and Radio Engineering*, **74**(15):1377-1390.
28. Bannister, P.R., (1999), Further examples of seasonal variations of ELF radio propagation parameters, *Radio Sci*. **34**(1):199–208.
29. Nickolaenko, A.P., (2008), ELF attenuation factor derived from distance dependence of radio wave amplitude propagation from an artificial source, *Telecommunications and Radio Engineering*, **67**(18):1621-1629.